International Journal of Bifurcation and Chaos, Vol. 23, No. 12 (2013) 1350199 (10 pages)

DOI: 10.1142/S021812741350199X

MULTISTABILITY IN A BUTTERFLY FLOW

CHUNBIAO LI* and J. C. SPROTT†
Department of Physics, University of Wisconsin–Madison, Madison, WI 53706, USA
**School of Information Science and Engineering, Southeast University, Nanjing 210096, P. R. China*
**Engineering Technology Research and Development Center of Jiangsu Circulation Modernization Sensor Network, Jiangsu Institute of Commerce, Nanjing 210007, P. R. China*
**chunbiaolee@gmail.com*
†*sprott@physics.wisc.edu*

Received June 5, 2013

A dynamical system with four quadratic nonlinearities is found to display a butterfly strange attractor. In a relatively large region of parameter space the system has coexisting point attractors and limit cycles. At some special parameter combinations, there are five coexisting attractors, where a limit cycle coexists with two equilibrium points and two strange attractors in different attractor basins. The basin boundaries have a symmetric fractal structure. In addition, the system has other multistable regimes where a pair of point attractors coexist with a single limit cycle or a symmetric pair of limit cycles and where a symmetric pair of limit cycles coexist without any stable equilibria.

Keywords: Multistability; coexisting attractor; attraction basin; butterfly attractor.

1. Introduction

Multistability and hidden attractors have been of recent interest because they pose a threat to practical engineering applications [Banerjee, 1997; Chizhevsky, 2000; Graham & Tél, 1986; Leonov *et al.*, 2011, 2012; Okafor *et al.*, 2010; Ray *et al.*, 2009; Sprott *et al.*, 2013]. In high-dimensional systems and in low-dimensional systems with multiple nonlinearities, coexisting attractors with their separate attracting basins are often unavoidable. In this paper, we consider a particular simple example of a three-dimensional autonomous flow with four quadratic terms and the following properties: (1) It has three equilibrium points. (2) In certain regions of parameter space, it has a symmetric multiwing strange attractor. (3) It has a broad region of parameter space where a symmetric pair of point attractors coexists with limit cycles of various structures and periodicities. (4) It has other regions with five coexisting attractors, where a symmetric pair of point attractors and a symmetric limit cycle coexist with either a symmetric pair of limit cycles or a symmetric pair of strange attractors. Also, the system has other regimes, where two, three, or four attractors coexist. (5) The basins of attraction have a symmetric fractal structure. In Sec. 2, we map out the dynamic regions in the two-dimensional bifurcation parameter space. In Sec. 3, we describe the butterfly attractor, its basic properties, and its route to chaos through a bifurcation diagram. In Sec. 4, we show examples of the coexisting attractors and their fractal basins. The last section is a discussion and conclusion.

2. A System with Four Quadratic Nonlinearities and Its Dynamical Regions

Inspired by the abundant dynamical behavior produced by polynomial nonlinearities and considering that many real dynamical systems have numerous nonlinear feedback loops, we consider a new three-dimensional system of first-order, autonomous, ordinary differential equations with four cross-product terms,

$$\begin{cases} \dot{x} = y + yz, \\ \dot{y} = -xz + yz, \\ \dot{z} = -az - xy + b. \end{cases} \tag{1}$$

System (1) is symmetric with respect to a 180° rotation about the z-axis, which can be shown by the coordinate transformation $(x, y, z) \to (-x, -y, z)$. When $a + b > 0$ and $a \neq 0$, system (1) possesses three real equilibrium points: $P_1 = (0, 0, b/a)$, $P_{2,3} = (\pm\sqrt{a+b}, \pm\sqrt{a+b}, -1)$. From the characteristic equation, $\lambda^3 + ((a^2 - b)/a)\lambda^2 + ((b^2 + ab - a^2b)/a^2)\lambda + ((b^2 + ab)/a) = 0$, the equilibrium point P_1 is stable provided $f(a, b) = (a^2 - b)^2 + ab + a^2b < 0$ according to the Routh–Hurwitz criterion. For other $a > 0$ and $b > 0$, the equilibrium P_1 is always unstable. Equilibrium points P_2 and P_3 are symmetric with respect to the z-axis, and their stability varies according to the parameters a and b. When they are unstable, they become the centers of two attracting scrolls, and when they are stable, they become a symmetric pair of coexisting point attractors. For a, $b < 0$, the system apparently does not have limit cycles or chaos, although it can have stable equilibria.

For most dynamical systems with quadratic nonlinearities, the bifurcation parameters are chosen as coefficients of the linear and constant terms. Since system (1) has seven terms, we expect it to have three adjustable parameters since four of the coefficients can be set to unity through a linear rescaling of x, y, z, and t. However, we consider a representative two-dimensional subset of the three-dimensional parameter space using parameters a and b in the third dimension. In this slice of parameter space, the regions of different dynamical behavior are shown in Fig. 1. In this plot, each pixel is calculated for a random initial condition taken from a Gaussian distribution with mean zero and unit variance, which accounts for the dotted regions that are candidates for coexisting attractors.

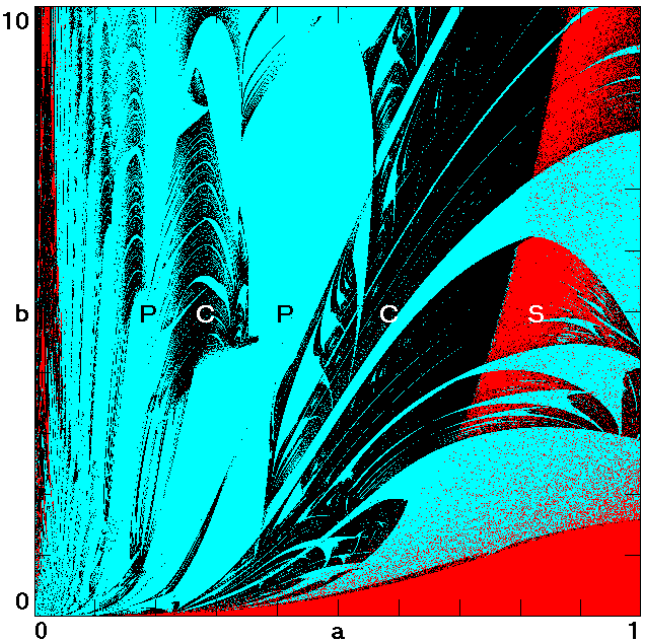

Fig. 1. Regions of different dynamical behaviors in the space of the bifurcation parameters a and b. The chaotic and transiently chaotic regions (C) are shown in black, the periodic regions (P) are shown in blue, and the stable equilibrium regions (S) are shown in red.

More nonlinear terms generally result in more complicated dynamical behavior as evidenced by Fig. 1 which shows a number of specific properties:

(1) Periodic solutions are the main behavior, with limit cycles occurring over much of the region, including numerous periodic windows and coexisting with point attractors.
(2) Periodic windows play an important role in the evolution of the butterfly flow. There are many evident periodic windows separating the chaotic regions into isolated strips or islands.
(3) There is a relatively broad region of parameter space in which the system has point attractors.
(4) The stability of the symmetric pair of equilibrium points $P_{2,3}$ accounts for some of the bifurcations on the right-hand side of the plot. From the characteristic equation for $P_{2,3}$ given by $\lambda^3 + (a+1)\lambda^2 + (2a+b)\lambda + 2(a+b) = 0$, the theoretical bifurcation boundary $b = \frac{2a^2}{1-a}$ shown in Fig. 2 divides the parameter space into regions with unstable saddle-foci and stable foci.
(5) The symmetry brings the possibility of a symmetric pair of coexisting attractors of the same type, which would not be evident in Fig. 1.

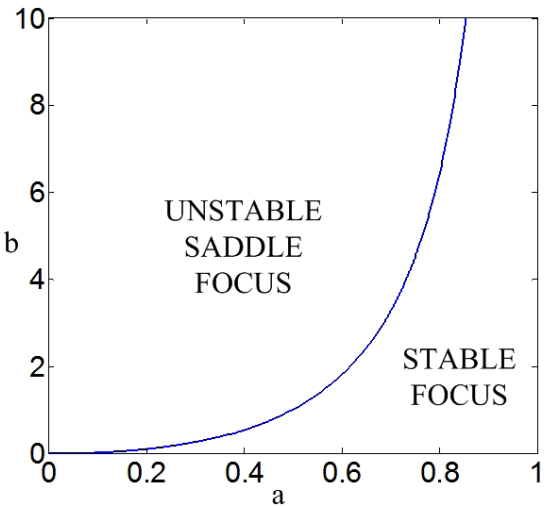

Fig. 2. The theoretical bifurcation boundary for the symmetric pair of foci.

(6) The dotted regions of red and blue indicate point attractors coexisting with one or two limit cycles.

(7) The dotted regions of red and black suggest a strange attractor coexisting with a symmetric pair of stable equilibrium points, but upon closer inspection, these regions are found to be only transiently chaotic [Dhamala & Lai, 1999], with the flow eventually attracting to one of the stable equilibria. The long transient is presumably a consequence of the presence of the two equilibria with their convoluted basins of attraction.

(8) The dotted regions of red, blue, and black indicate coexisting strange attractors, limit cycles and point attractors, only one other example of which has been reported with three such attractors [Sprott *et al.*, 2013], whereas the present case has five coexisting attractors of three types.

3. Butterfly Chaotic Attractor and Its General Properties

For $a = 0.6$ and $b = 3$, system (1) is chaotic with a symmetric chaotic attractor as shown in Fig. 3. The attractor exhibits four small butterfly wings embedded in an outer double-wing. The Lyapunov exponents for this case are $L_1 = 0.1528$, $L_2 = 0$, $L_3 = -0.7828$, and the Kaplan–Yorke dimension is $D_{KY} = 2 - \lambda_1/\lambda_3 = 2.1952$.

For $a = 0.6$ and $b = 3$, the corresponding equilibrium points are $P_1 = (0, 0, 5)$ and $P_{2,3} = (\pm\sqrt{3.6}, \pm\sqrt{3.6}, -1)$. For the equilibrium $P_1 = (0, 0, 5)$, system (1) is linearized, and the Jacobian matrix is given by

$$J_1 = \begin{pmatrix} 0 & 1+z & y \\ -z & z & y-x \\ -y & -x & -a \end{pmatrix} = \begin{pmatrix} 0 & 6 & 0 \\ -5 & 5 & 0 \\ 0 & 0 & -0.6 \end{pmatrix}. \tag{2}$$

From $|\lambda I - J_1| = 0$, the resulting eigenvalues of the Jacobian matrix J_1 are obtained as $\lambda_1 = -0.6$, $\lambda_{2,3} = 2.5 \pm 4.8734i$. Here λ_1 is a negative real

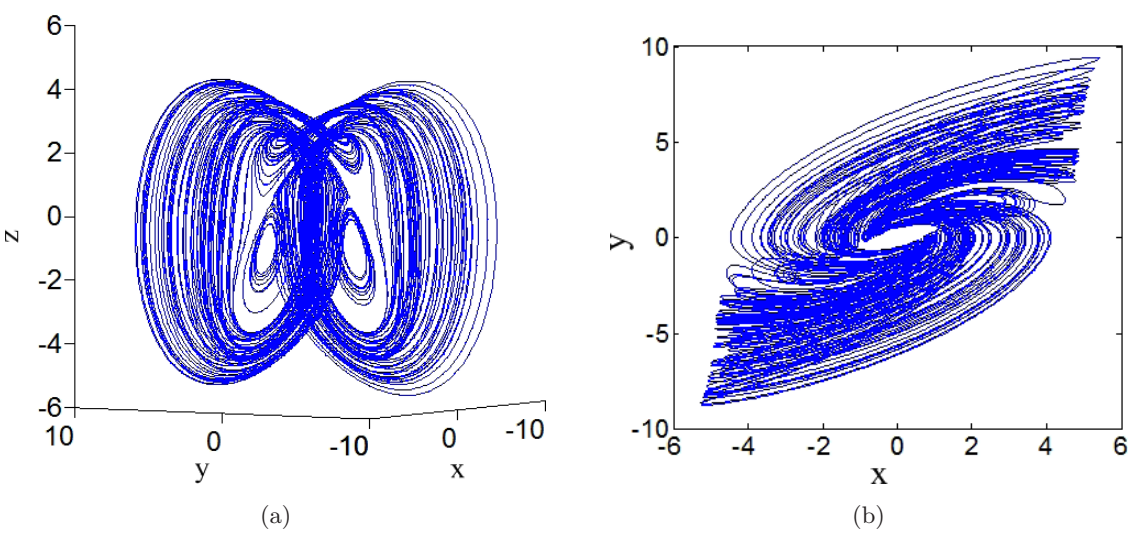

(a) (b)

Fig. 3. Butterfly chaotic attractor from Eq. (1) with $a = 0.6$, $b = 3$ for $(x_0, y_0, z_0) = (1, -1, 1)$: (a) three-dimensional view, (b) projection on x–y plane, (c) projection on x–z plane and (d) projection on y–z plane.

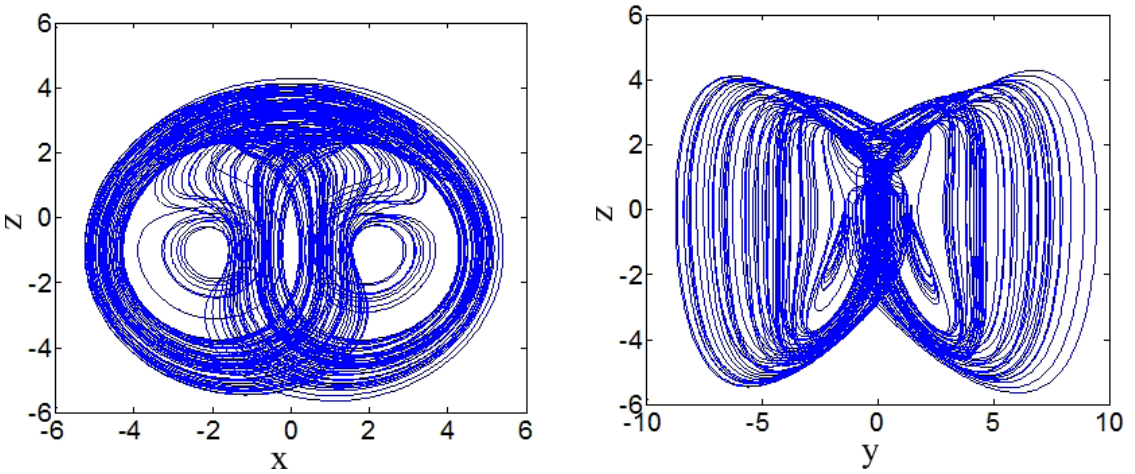

(c) (d)

Fig. 3. (*Continued*)

number, and λ_2, λ_3 are a pair of complex conjugate eigenvalues with positive real parts. Consequently, the equilibrium P_1 is a saddle-focus, and system (1) is unstable at the P_1 equilibrium point. For the equilibria $P_{2,3} = (\pm\sqrt{3.6}, \pm\sqrt{3.6}, -1)$, the resulting eigenvalues of the Jacobian matrix are $\lambda_1 = -1.6687, \lambda_{2,3} = 0.0344 \pm 2.0769i$. The resulting eigenvalues of the Jacobian matrix also share a negative real number and a pair of complex conjugate eigenvalues with positive real parts. Consequently, the equilibria $P_{2,3}$ are both saddle-foci. Therefore, system (1) is unstable at these three equilibrium points, and which results in the butterfly attractor.

The plot of the dynamical regions shows that embedded periodic windows play an important role in the evolution of the butterfly flow. As shown in Figs. 4 and 5, after several periodic windows and with an increase in limit cycles, the amplitude of the chaotic signal increases, and the butterfly flow expands its size as the limit cycles open up.

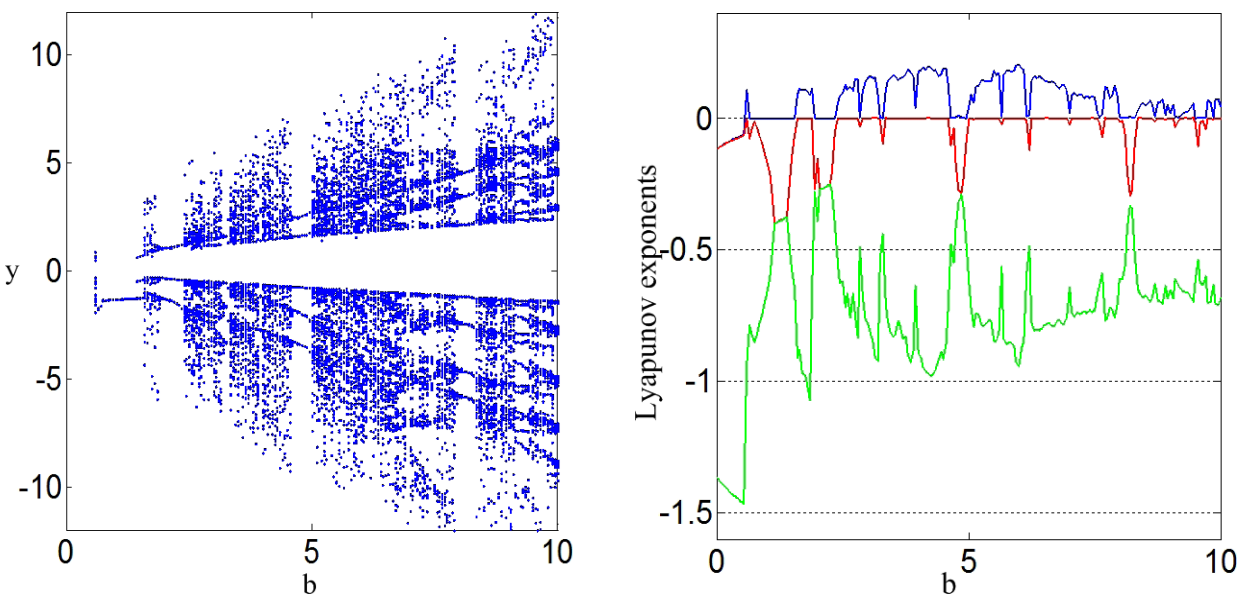

(a) (b)

Fig. 4. The dynamical behavior for $a = 0.6$ as b varies for $(x_0, y_0, z_0) = (1, -1, 1)$: (a) the value of y at $x = 0$ and (b) the Lyapunov exponents.

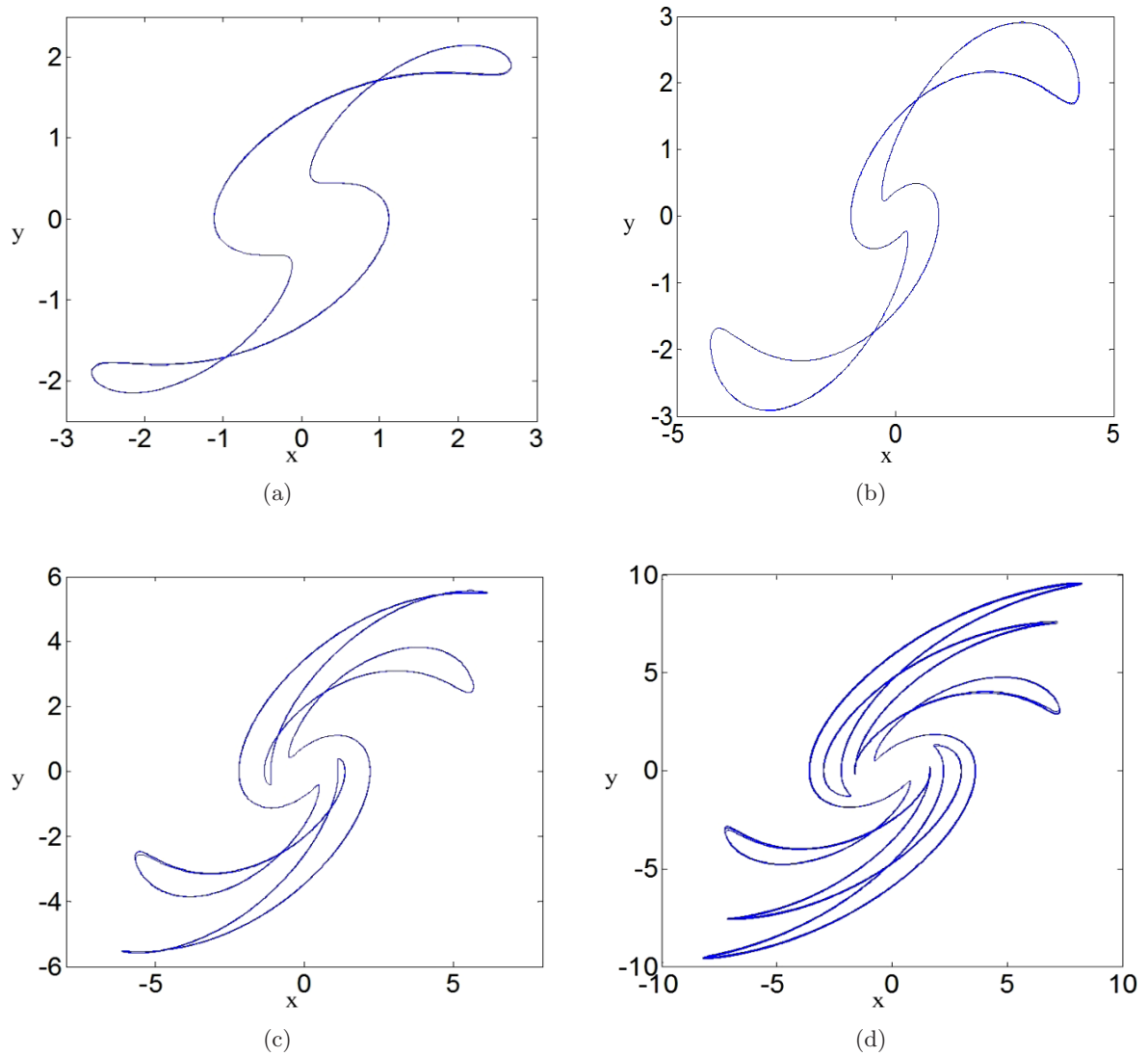

Fig. 5. Projection on the x–y plane of the trajectory in various periodic windows with $a = 0.6$ for $(x_0, y_0, z_0) = (1, -1, 1)$: (a) $b = 1$, (b) $b = 2.2$, (c) $b = 4.8$ and (d) $b = 8.2$.

4. Coexisting Attractors

As mentioned above, coexisting attractors are the most significant feature of the system. There is a relatively large parameter space of coexisting attractors located on the right side of Fig. 1 where a symmetric pair of point attractors coexists with other attractors. To compare with the region without coexisting point attractors and to explore more attractor-coexisting regimes, we select an additional combination of parameters. As shown in Fig. 6, the main coexisting regime is a symmetric pair of point attractors coexisting with a symmetric limit cycle. However, there are several other coexisting regimes as shown in Table 1. The basic coexisting attractors are the symmetric pair of stable foci. For some parameter combinations, the point attractors can coexist with a symmetric and/or symmetric pair of limit cycles, while on the other side of parameter space according to Fig. 2, a symmetric or symmetric pair of limit cycles exist without stable equilibrium. In some parameter regions, the system also has coexisting point attractors, limit cycles and chaos. The corresponding phase portraits of the coexisting attractors in the x–z plane are shown in Fig. 6.

The symmetric pair of point attractors is the basic coexisting regime in this butterfly flow. Figure 6(a) shows the trajectory approaching these point attractors from two different initial conditions. The coexisting periodic trajectories have a wide variety of periods and structures as shown in

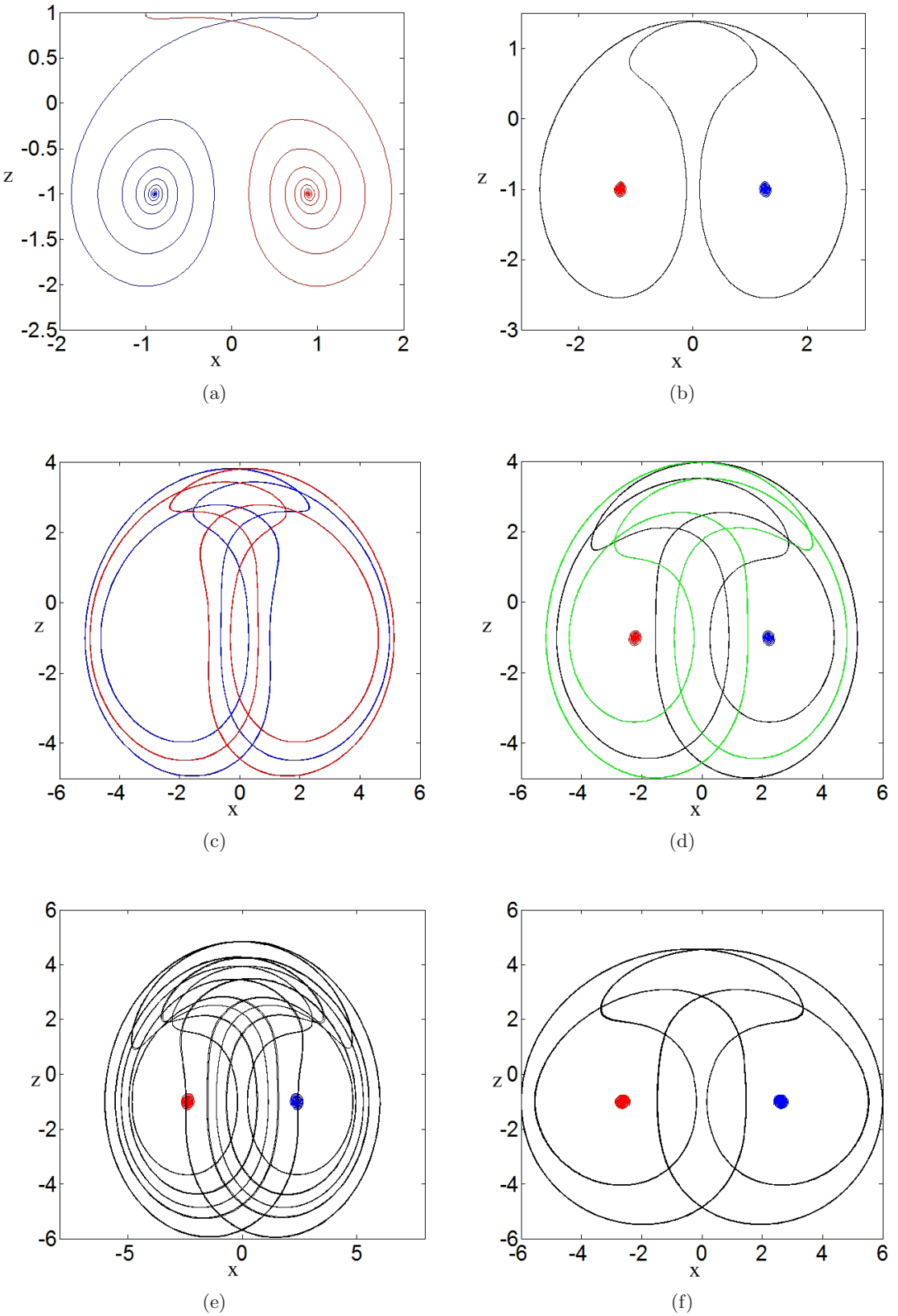

Fig. 6. Phase portrait of coexisting attractors in the x–z plane: (a) $a = 0.6$, $b = 0.2$, (b) $a = 0.6$, $b = 1$, (c) $a = 0.6$, $b = 3.3$, (d) $a = 0.9$, $b = 4$, (e) $a = 0.9$, $b = 4.8$, (f) $a = 0.9$, $b = 6$, (g) $a = 0.55$, $b = 0.8$ and (h) $a = 0.55$, $b = 0.85$ (red and blue, green and black with symmetric initial conditions).

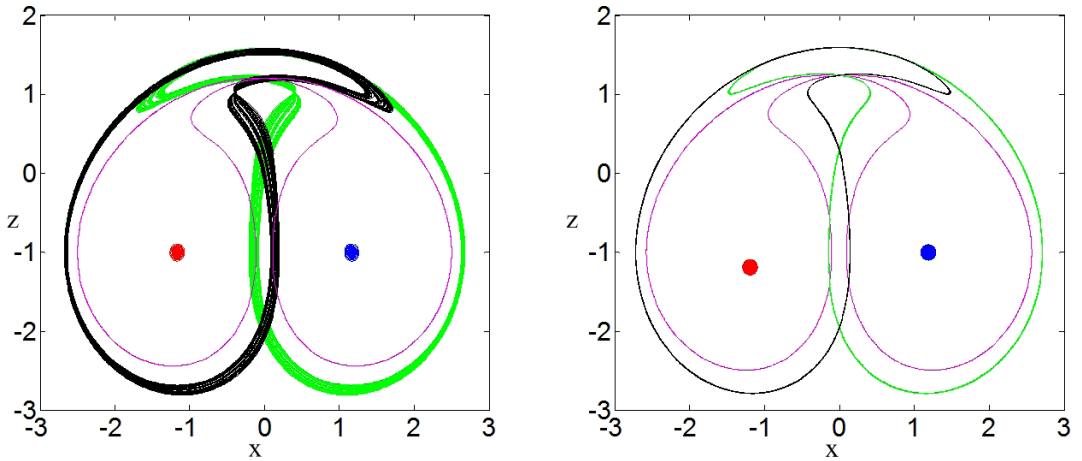

(g) (h)

Fig. 6. (*Continued*)

Figs. 6(b)–6(f). On either side of the theoretical boundary in parameter space according to Fig. 2, the limit cycles have different coexisting modes according to the stability of the symmetric pair of equilibrium points. In the area of unstable saddle-foci, a symmetric pair of limit cycles coexists without coexisting point attractors as shown in Fig. 6(c). For $a = 0.55$ and $b = 0.8$, a symmetric limit cycle coexists with a symmetric pair of stable foci and a symmetric pair of strange attractors as shown in Fig. 6(g). The Lyapunov exponents for the strange attractors are $L_1 = 0.0508$, $L_2 = 0$, $L_3 = -0.4489$. For $a = 0.55$ and $b = 0.85$, three limit cycles coexist with a symmetric pair of stable foci as shown in Fig. 6(h).

The basins of attraction of the different attracting sets provide more information about the coexisting attractors, which are defined as the set of initial conditions whose trajectories converge to the respective attractor. For $a = 0.9$ and $b = 4$, where a symmetric pair of point attractors coexists with a symmetric pair of limit cycles in Fig. 6(d), the basins in the $z = -1$ plane are shown in Fig. 7. The basins of the two point attractors are indicated

Table 1. Coexisting attractors for various parameters.

Regimes	Parameters	Initial Conditions	Lyapunov Exponents	Attractor Dimensions
Symmetric pair of point attractors	$a = 0.6$, $b = 0.2$	$(\pm 1, 0, 1)$	$(-0.0939, -0.0946, -1.4104)$	0
Two point attractors with a symmetric limit cycle	$a = 0.6$, $b = 1$	$(\pm 1, \pm 2, -1)$ $(1, 0, -1)$	$(-0.0353, -0.0356, -1.5291)$ $(0, -0.1616, -0.6657)$	0 1
Symmetric pair of limit cycles	$a = 0.6$, $b = 3.3$	$(\pm 1, 0, -1)$	$(0, -0.0944, -0.4522)$	1
Two point attractors with a symmetric pair of limit cycles	$a = 0.9$, $b = 4$	$(\pm 6.5, \mp 1, 1)$ $(\pm 1, \mp 1, 1)$	$(-0.0660, -0.0709, -1.7623)$ $(0, -0.1107, -0.6636)$	0 1
Two point attractors with a symmetric limit cycle	$a = 0.9$, $b = 4.8$	$(\pm 6.5, \mp 1, 1)$ $(\pm 1, \mp 1, 1)$	$(-0.0572, -0.0593, -1.7834)$ $(0, -0.1139, -0.6161)$	0 1
Two point attractors with a symmetric limit cycle	$a = 0.9$, $b = 6$	$(\pm 6.5, \mp 1, 1)$ $(\pm 1, \mp 1, 1)$	$(-0.0451, -0.0465, -1.8084)$ $(0, -0.1843, -0.7039)$	0 1
Two point attractors with a limit cycle and a symmetric pair of strange attractors	$a = 0.55$, $b = 0.8$	$(\pm 1, \pm 1, -1)$ $(0.8, 0.3, 0.5)$ $(\pm 0.4, 0, 1)$	$(-0.0296, -0.0299, -1.4904)$ $(0, -0.3550, -0.4618)$ $(0.0508, 0, -0.4489)$	0 1 2.1132
Two point attractors with a limit cycle and a symmetric pair of limit cycles	$a = 0.55$, $b = 0.85$	$(\pm 1, \pm 1, -1)$ $(0.8, 0.3, 0.5)$ $(\pm 0.4, 0, 1)$	$(-0.0264, -0.0268, -1.4967)$ $(0, -0.4030, -0.4041)$ $(0, -0.0204, -0.3602)$	0 1 1

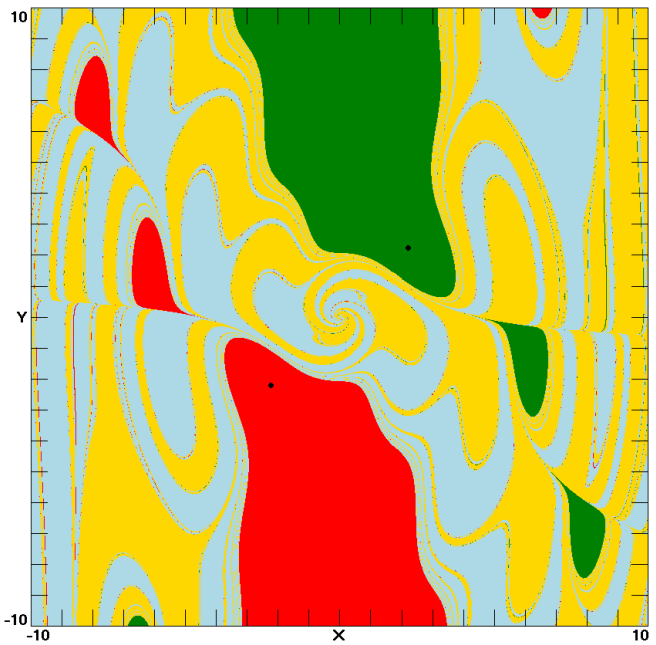

Fig. 7. Cross-section for $z = -1$ of the basins of attraction for the limit cycles (light blue and yellow) and the symmetric pair of point attractors (red and green) of system (1) at $a = 0.9$, $b = 4$.

by red and green, respectively, and the basin of the limit cycles are shown in light blue and yellow. The basins have the expected symmetry about the z-axis and a fractal boundary.

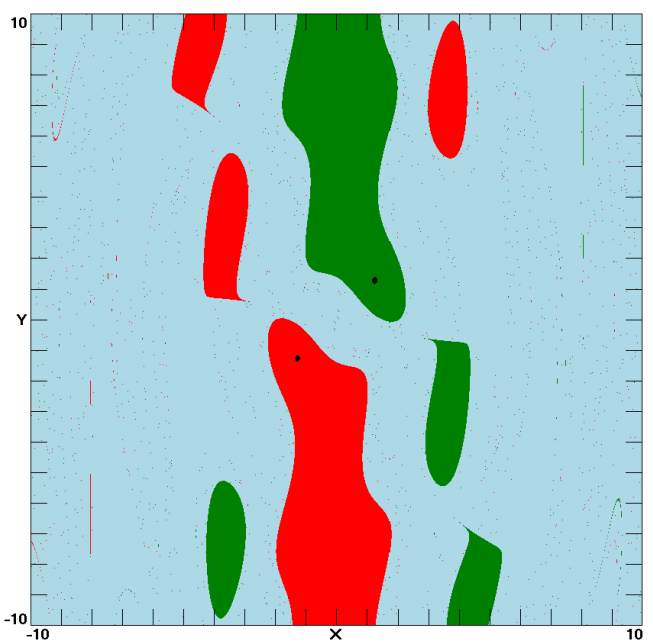

Fig. 8. Cross-section for $z = -1$ of the basins of attraction for the symmetric pair of point attractors (red and green) and the limit cycle (light blue) of system (1) at $a = 0.6$, $b = 1$.

For the regime of three coexisting attractors, the case $a = 0.6$ and $b = 1$, where a symmetric pair of point attractors coexists with a limit cycle whose trajectories are shown in Fig. 6(b) with basins of attraction as shown in Fig. 8.

For the regime of five coexisting attractors, with $a = 0.55$ and $b = 0.8$, the basins of attraction are shown in Fig. 9, where a symmetric limit cycle coexists with a symmetric pair of point attractors and a symmetric pair of strange attractors whose trajectories are shown in Fig. 6(g). Furthermore, it can be seen that the two coexisting strange attractors are linked together as shown in Fig. 10. However, it is verified that there is no continuous chaotic path in ab-space from the region with a symmetric pair of strange attractors to the region with a single strange attractor. What appears to happen is that the pair of strange attractors are destroyed through a sequence of inverse period doublings to a symmetric pair of limit cycles which then period double and abruptly lose their stability while a symmetric strange attractor is born. This is not to say that there are no other regions in parameter space where two strange attractors merge into one, but this may require considering the ignored third parameter.

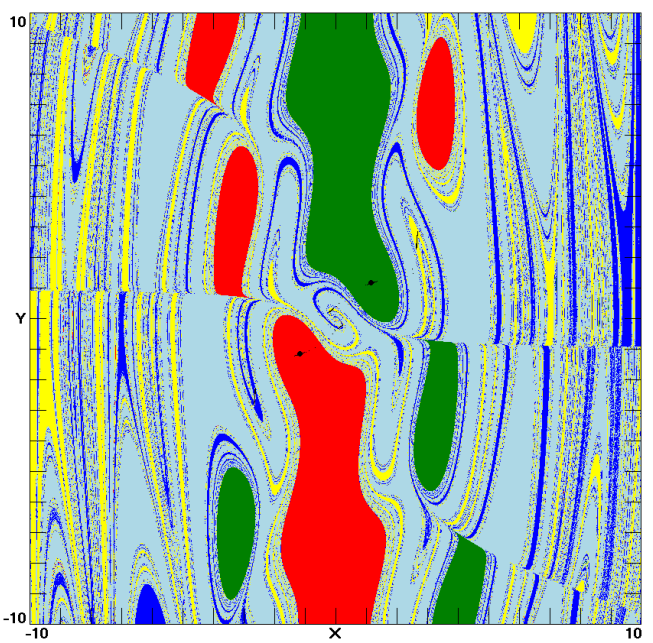

Fig. 9. Cross-section for $z = -1$ of the basins of attraction for the symmetric pair of point attractors (red and green), the symmetric limit cycle (light blue) and a symmetric pair of strange attractors (yellow and dark blue) of system (1) at $a = 0.55$, $b = 0.8$.

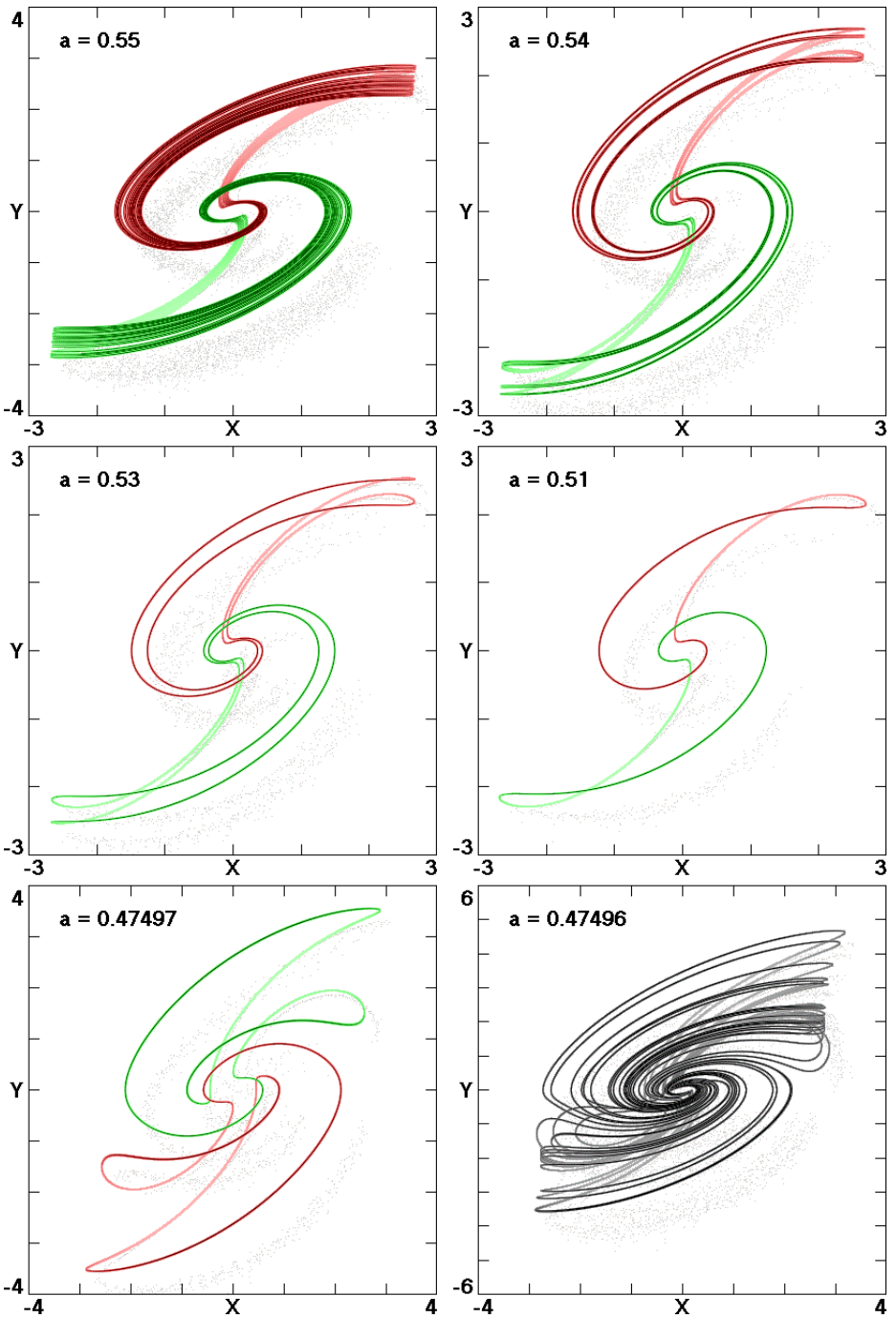

Fig. 10. Linked attractors in the x–y plane of system (1) at $b = 0.8$ and its evolution to a symmetric strange attractor.

5. Discussion and Conclusion

There is a relationship between multistability and equilibrium. The variation of bifurcation parameters will change the property of the equilibrium points and may embed corresponding point attractors in dynamical systems depending on the stability of the equilibrium and attractor basins. Here by the exploration of a new three-dimensional autonomous butterfly flow with four cross-product terms, we show that the embedded stable equilibria can coexist with other attractors, and their unstable states can give birth to corresponding attracting scrolls. The proposed butterfly flow is a good example of three, four and even five coexisting attractors, where a symmetric pair of point attractors coexists with a symmetric limit cycle and with a symmetric pair of strange attractors or limit cycles. We

conclude that the equilibrium points have different dynamical effects depending on their stability and the system structure.

Acknowledgments

This work was supported by the Jiangsu Overseas Research and Training Program for University Prominent Young and Middle-aged Teachers and Presidents, the 4th 333 High-level Personnel Training Project (Su Talent [2011] No.15) and Qing Lan Project of Jiangsu Province, the National Science Foundation for Postdoctoral General Program and Special Founding Program of People's Republic of China (Grant No. 2011M500838 and Grant No. 2012T50456) and Postdoctoral Research Foundation of Jiangsu Province (Grant No. 1002004C).

References

Banerjee, S. [1997] "Coexisting attractors, chaotic saddles, and fractal basins in a power electronic circuit," *IEEE Trans. Circuits Syst.-I*: *Fund. Th. Appl.* **44**, 847–849.

Chizhevsky, V. N. [2000] "Coexisting attractors in a CO_2 laser with modulated losses," *J. Opt. B*: *Quant. Semiclass. Opt.* **2**, 711–717.

Dhamala, M. & Lai, Y. C. [1999] "Controlling transient chaos in deterministic flows with applications to electrical power systems and ecology," *Phys. Rev. E* **59**, 1646–1655.

Graham, R. & Tél, T. [1986] "Nonequibrium potential for coexisting attractors," *Phys. Rev. A* **33**, 1322–1337.

Leonov, G. A., Vagaitsev, V. I. & Kuznetsov, N. V. [2011] "Localization of hidden Chua's attractors," *Phys. Lett. A* **375**, 2230–2233.

Leonov, G. A., Vagaitsev, V. I. & Kuznetsov, N. V. [2012] "Hidden attractor in smooth Chua systems," *Physica D* **241**, 1482–1486.

Okafor, N., Zahawi, B., Giaouris, D. & Banerjee, S. [2010] "Chaos, coexisting attractors, and fractal basin boundaries in DC drives with full-bridge converter," *IEEE Int. Symp. Proc. Circuits Syst.* (*ISCAS*), pp. 129–132.

Ray, A., Ghosh, D. & Chowdhury, A. R. [2009] "Topological study of multiple coexisting attractors in the nonlinear system," *J. Phys. A*: *Math. Theor.* **42**, 385102.

Sprott, J. C., Wang, X. & Chen, G. [2013] "Coexistence of point, periodic and strange attractors," *Int. J. Bifurcation and Chaos* **23**, 1350093.